

Characterisation of the elastic properties of porous foams

Laurens Boeckx, Luc Kelders, Philippe Leclaire, Poonam Khurana, Walter Lauriks

► To cite this version:

Laurens Boeckx, Luc Kelders, Philippe Leclaire, Poonam Khurana, Walter Lauriks. Characterisation of the elastic properties of porous foams. 12th International Congress on Sound and Vibration 2005 (ICSV 12), Jul 2005, Lisbonne, Portugal. pp.268-275. hal-01326046

HAL Id: hal-01326046

<https://hal.archives-ouvertes.fr/hal-01326046>

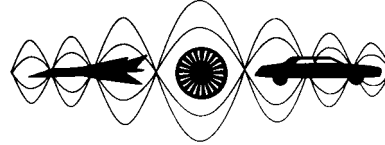
Submitted on 3 Jun 2016

HAL is a multi-disciplinary open access archive for the deposit and dissemination of scientific research documents, whether they are published or not. The documents may come from teaching and research institutions in France or abroad, or from public or private research centers.

L'archive ouverte pluridisciplinaire **HAL**, est destinée au dépôt et à la diffusion de documents scientifiques de niveau recherche, publiés ou non, émanant des établissements d'enseignement et de recherche français ou étrangers, des laboratoires publics ou privés.



Distributed under a Creative Commons Attribution| 4.0 International License



**Twelfth International Congress
on Sound and Vibration**

CHARACTERISATION OF THE ELASTIC PROPERTIES OF POROUS FOAMS

L. Boeckx, L.Kelders, P.Leclaire, P.Khurana, W. Lauriks

Laboratory for acoustics and thermal physics;
Catholic University Leuven, Celestijnenlaan 200D, B-3001 Heverlee, Belgium
(e-mail address of lead author) Walter.Lauriks@fys.kuleuven.ac.be

Abstract

An experimental method for measuring the elastic constants of poroelastic foams as a function of frequency is presented. The method is based on the measurement of phase velocities of guided acoustic waves in a slab of the material. Standing waves are generated in the material and the phase velocities are evaluated using the spatial Fourier Transform of the displacement profile of the upper surface. The displacement is measured with the help of a Laser Doppler vibrometer along a line corresponding to the direction of propagation of plane surface waves. The spatial Fourier Transform provides the wave numbers and the phase velocities are obtained from the relationship between wave number and frequency. The phase velocity of several guided modes could be measured in highly porous foams saturated by air. The modes were also studied theoretically and from the theoretical and experimental results, it was possible to determine the frequency behavior of the real part of the shear modulus and in a frequency range higher than the traditional methods. Experimental results concerning guided waves in isotropic porous materials tend to suggest that information about the anisotropy of the elastic matrix can also be obtained.

INTRODUCTION

Biot (1956) proposed the theory of propagation of acoustic waves in isotropic poroelastic homogeneous medium. Such a material supports one additional slow longitudinal wave which is diffusive at low frequencies but propagative at high frequencies and carries useful information on some of the porous material properties. However, the main limitation of the model is the lack of data on the dynamic

rigidities of the porous frame. Some of the classical methods for determining the elastic parameters are limited in frequency range. In the past few years, new experimental methods have been proposed to characterize the elastic properties of foams or fibrous materials used in the field of acoustics. A new method for measuring the shear modulus of air-filled porous materials based on the propagation of Rayleigh waves in thick layers was recently proposed by Allard et al. [1] and provided useful information above 3 kHz. More recently, Allard et al. [2] have proposed a new method of measurement in thinner samples in which Biot's shear wave is excited. This method is based on the effect of the resonance of the porous frame around the quarter shear wavelength on the pole of the reflection coefficient.

Foams may be anisotropic, especially orthotropic or transverse isotropic. Surface wave velocity has been proved to be the useful tool in determining the dynamic properties of saturated porous materials. Surface modes in liquid saturated media are studied by a number of researchers (Deresiewicz [3], Feng and Johnson [4], Kelders [5], Lauriks [6] and Smith et al [7]). Recently the detection of guided waves in a layer of sound absorbing porous material of finite thickness has been reported at Kyoto by Boeckx et al. [8]. A new experimental method is proposed in this article for the determination of the modes of propagation in a plate of finite sizes in the Lamb conditions. This method, characterized by an increased signal to noise ratio and measurement accuracy, is based on the generation of standing waves in the layer of porous material. Theoretical results on guided waves in transverse isotropic poroelastic solid (TIPS) are also presented.

BIOT'S THEORY

Following Biot (1956) [9], the equations of motion for transverse isotropic poroelastic solid are given by

$$\begin{aligned} \tau_{i1,1} + \tau_{i2,2} + \tau_{i3,3} &= \rho \ddot{u}_i + \rho_f \ddot{W}_i, & (i, j = 1, 2, 3), \\ -(p_f)_{,i} &= \rho_f \ddot{u}_i + \frac{\hat{c}_i \rho_f}{\beta} \ddot{W}_i + F b_i \dot{W}_i, \end{aligned} \quad (1)$$

where β is porosity, τ_{ij} are the total stress components acting on both the solid and fluid phases, p_f is the pore fluid pressure, ρ_f is the mass density of the fluid, ρ is the bulk density of the porous material, u_i , U_i are the components of the average displacements of the solid and fluid phases respectively, $\dot{W}_i = \beta(\dot{U}_i - \dot{u}_i)$ are the components of fluid-discharge velocity. The viscodynamic operator $F(B^2\omega)$ represents the friction between the solid and fluid phases. For circular pores, $\hat{b}_i = \frac{\xi}{k_i}$,

where ξ and k_i are the viscosity and permeability of the pore fluid, respectively. For cylindrical pores, the permeability is given by $k_i = \left(\frac{8}{\bar{a}^2}\right)\delta_i$, where \bar{a} is the pore size and δ_i is the shape factor and its value is one for circular cylindrical pores.

$$F(B^2\omega) = \left(1 + \frac{\sigma\beta}{jB^2\omega\rho_f\hat{c}_i} G_j(B^2\omega)\right)^{-1}, \quad G_j(\omega) = \left(1 + \frac{4\hat{c}_i^2 j\xi\rho_f\omega B^2}{\sigma^2\Lambda^2\beta^2}\right), \quad \Lambda = \frac{1}{c} \left(\frac{8\xi\hat{c}_i}{\sigma\beta}\right)$$

Where σ is the flow resistivity, B^2 is the Prandtl number and Λ the characteristic length for which the value is given for cylindrical pores.

The \hat{c}_i in equations (1) are experimentally determined parameters that account for the fact that not all of the fluid moves in the direction of macroscopic pressure gradient because of the shape and orientation of the interstitial cavities. In the case of straight pores, these constants are unity.

Following Biot, (1962) [10], the constitutive equations for the transversely isotropic porous solid with symmetry about z-axis, are

$$\begin{aligned} \tau_{xx} &= 2B_1 e_{xx} + B_2 (e_{xx} + e_{yy}) + B_3 e_{zz} + B_6 \zeta, \\ \tau_{yy} &= 2B_1 e_{yy} + B_2 (e_{xx} + e_{yy}) + B_3 e_{zz} + B_6 \zeta, \\ \tau_{zz} &= B_4 e_{zz} + B_3 (e_{xx} + e_{yy}) + B_7 \zeta, \\ \tau_{yz} &= 2B_5 e_{yz}, \quad \tau_{zx} = 2B_5 e_{zx}, \quad \tau_{xy} = 2B_1 e_{xy}, \\ p_f &= B_6 (e_{xx} + e_{yy}) + B_7 e_{zz} + B_8 \zeta, \quad \text{where } e_{ij} = \frac{1}{2} \left(\frac{\partial u_i}{\partial x_j} + \frac{\partial u_j}{\partial x_i} \right). \end{aligned} \quad (2)$$

B_1, \dots, B_8 are the eight elastic constants for transversely isotropic porous solid (TIPS). The constants for isotropic solids can be obtained by following substitutions $B_1 = B_5$, $B_2 = B_3$, $B_7 = B_6$, $B_4 = B_2 + 2B_1$.

The plane harmonic wave solutions of equations (1) are written in the form

$$\begin{aligned} u_x &= a_1 \exp\left(i\omega\left(t - \frac{x}{c} - qz\right)\right), \quad u_z = a_3 \exp\left(i\omega\left(t - \frac{x}{c} - qz\right)\right), \\ U_x &= b_1 \exp\left(i\omega\left(t - \frac{x}{c} - qz\right)\right), \quad U_z = b_3 \exp\left(i\omega\left(t - \frac{x}{c} - qz\right)\right), \end{aligned} \quad (3)$$

where a_1 , a_3 , b_1 and b_3 are the wave amplitudes. Substituting these expressions in the equations (1) through the equations (2), we obtain a set of four equations, nontrivial solution of which is possible only if

$$T_0 q^6 + T_1 q^4 + T_2 q^2 + T_3 = 0. \quad (4)$$

The expressions for T_0 , T_1 , T_2 and T_3 are given in Appendix and are well described by Sharma and Gogna [11].

The roots of the equation (4) are, in general, complex. We denote these roots by $q(n)$, $n = 1, 2, \dots, 6$. Three roots with positive real parts correspond to the waves traveling in the positive z-direction (down going waves) and the other three roots with negative real parts correspond to the waves traveling in the negative z-direction (up going waves). We order the six roots $q(n)$, $n = 1, 2, \dots, 6$ such that $q(1)$, $q(2)$, $q(3)$ correspond to the three up going waves, namely quasi- P_f , quasi- P_s and quasi- SV waves

respectively; and $q(6)$, $q(5)$ and $q(4)$ correspond to the down going quasi- P_f, quasi- P_s and quasi- SV waves respectively.

The displacements associated with the up going and down going quasi-body waves in transverse isotropic porous layer (TIPS) are

$$\begin{aligned} u_x &= \sum_{n=1}^6 f(n) a_1(n) \exp\left(i\omega\left(t - \frac{x}{c} - q(n)z\right)\right), \quad u_z = \sum_{n=1}^6 f(n) a_3(n) \exp\left(i\omega\left(t - \frac{x}{c} - q(n)z\right)\right), \\ W_x &= \sum_{n=1}^6 f(n) b_1(n) \exp\left(i\omega\left(t - \frac{x}{c} - q(n)z\right)\right), \quad W_z = \sum_{n=1}^6 f(n) b_3(n) \exp\left(i\omega\left(t - \frac{x}{c} - q(n)z\right)\right), \end{aligned} \quad (5)$$

where $f(n)$ are relative excitation factors.

A. TIPS plate backed by rigid surface

First we study the case when a layer of transversely isotropic poroelastic solid of thickness H is lying on a rigid surface. The boundary conditions at the free surface $z = 0$ are the vanishing of stress components τ_{zz} , τ_{zx} and p_f i.e.

$$\tau_{zz} = \tau_{zx} = p_f = 0. \quad (6)$$

And at the surface $z = H$ which is backed by rigid surface, boundary conditions are given by the vanishing of displacement components u_x , u_z and W_z i.e.

$$u_x = u_z = W_z = 0. \quad (7)$$

Using the relations (2) and the expressions (5), the boundary conditions (6) and (7) yields the dispersion equation for the TIPS plate backed by rigid substrate on one end in the form of following determinant

$$\begin{vmatrix} a_1(1)\exp(-\theta_1) & a_1(2)\exp(-\theta_1) & a_1(3)\exp(-\theta_1) & a_1(3)\exp(\theta_1) & a_1(2)\exp(\theta_2) & a_1(1)\exp(\theta_1) \\ a_3(1)\exp(-\theta_1) & a_3(2)\exp(-\theta_1) & a_3(3)\exp(-\theta_1) & -a_3(3)\exp(\theta_1) & -a_3(2)\exp(\theta_2) & -a_3(1)\exp(\theta_1) \\ b_3(1)\exp(-\theta_1) & b_3(2)\exp(-\theta_1) & b_3(3)\exp(-\theta_1) & -b_3(3)\exp(\theta_1) & -b_3(2)\exp(\theta_2) & -b_3(1)\exp(\theta_1) \\ C_1 & C_2 & C_3 & -C_3 & -C_2 & -C_1 \\ D_1 & D_2 & D_3 & D_3 & D_2 & D_1 \\ P_1 & P_2 & P_3 & P_3 & P_2 & P_1 \end{vmatrix} = 0, \quad (8)$$

where

$$\begin{aligned} \theta_n &= i\omega q(n)H, \quad C_n = L[a_1(n)r(n) + ia_3(n)], \\ D_n &= [Qa_3(n) + Rb_3(n)]r(n) + i[Ma_1(n) + Rb_1(n)] \\ P_n &= [Ca_3(n) + Qb_3(n)]r(n) + i[Fa_1(n) + Qb_1(n)], \quad r(n) = cq(n). \end{aligned}$$

B. Free TIPS Plate

Next is the case when the TIPS plate is free on both sides. The boundary conditions in this case are the vanishing of stresses τ_{zz} , τ_{zx} and p_f at the surface $z = 0$ as well as at $z = H$ which gives the determinant equation

$$\begin{vmatrix} C_1 \exp(-\theta_1) & C_2 \exp(-\theta_1) & C_3 \exp(-\theta_1) & -C_3 \exp(\theta_1) & -C_2 \exp(\theta_2) & -C_1 \exp(\theta_1) \\ D_1 \exp(-\theta_1) & D_2 \exp(-\theta_1) & D_3 \exp(-\theta_1) & D_3 \exp(\theta_1) & D_2 \exp(\theta_2) & D_1 \exp(\theta_1) \\ P_1 \exp(-\theta_1) & P_2 \exp(-\theta_1) & P_3 \exp(-\theta_1) & P_3 \exp(\theta_1) & P_2 \exp(\theta_2) & P_1 \exp(\theta_1) \\ C_1 & C_2 & C_3 & -C_3 & -C_2 & -C_1 \\ D_1 & D_2 & D_3 & D_3 & D_2 & D_1 \\ P_1 & P_2 & P_3 & P_3 & P_2 & P_1 \end{vmatrix} = 0. \quad (9)$$

EXPERIMENTAL SETUP AND PRINCIPLE

The experimental principle for studying guided waves in poro-elastic plates is shown in figure 1. The experimental setups and principles are also discussed by L. Boeckx et al. [12, 13]. A setup for studying the guided waves in a poro-elastic plate backed by rigid surface is presented on the left-hand side. Guided waves in a free poro-elastic plate can be investigated by the experimental setup presented in the right-hand side of figure 1. An electro dynamical shaker was used as a source. An aluminum plate was attached to the shaker to realize a line source. The shaker was fed with a stepped sinusoidal signal provided by the function generator unit of an SRS SR780 2 channel signal analyzer. The frequency of the sinusoidal signal was used as a reference for the lock-in amplifier of the SRS analyzer. A laser Doppler vibrometer detected the normal displacement component of the wave motion induced by the shaker. Patches of reflective tape were applied to the porous plate to realize reflection from the upper surface of the plate. A rigid ending was applied in both situations to eliminate partial reflection from the lateral boundaries of the porous plate. The rigid ending was a heavy metal plate at which perfect reflection of the guided waves could occur. It was attempted to realize a plate with infinite lateral dimensions using these rigid endings. When the plate was backed by a rigid substrate (left part of figure 1) the excitation region was opposite to the rigid ending of the porous plate. For the free condition (right part of figure 1) the excitation region was in the middle of the plate. Although a poro-elastic plate mounted in free conditions is easier to excite and offers a symmetrical displacement pattern, it can not always be realized. Most of the sound absorbing foams are very soft and therefore sagging effects would occur when mounted in free conditions. An investigation of the guided waves in a poro-elastic plate backed by a rigid substrate therefore offers a valuable and interesting alternative.

The normal displacement of the surface of the plate was measured for each driving frequency. The measurement point was allowed to move along a line parallel to the direction in which the plane waves propagate. The laser beam at the output of the laser Doppler vibrometer was collimated and a mirror/lens arrangement, which was mounted on a positionable arm, insured that the beam was always focused on the surface of the material at any position of the beam. A typical step size of the measurement is between 1 up to 5 mm and the length of the samples was typically around 1m. Due to the perfect reflection of the guided waves at the rigid endings an interference pattern arises. This standing wave pattern is measured along a direction parallel to the direction in which the plane surface waves propagate. The periodicity

of the standing wave pattern is determined by the guided waves which are allowed to propagate at the driving frequency. Measured standing wave patterns were Fourier transformed to obtain the spatial spectrum.

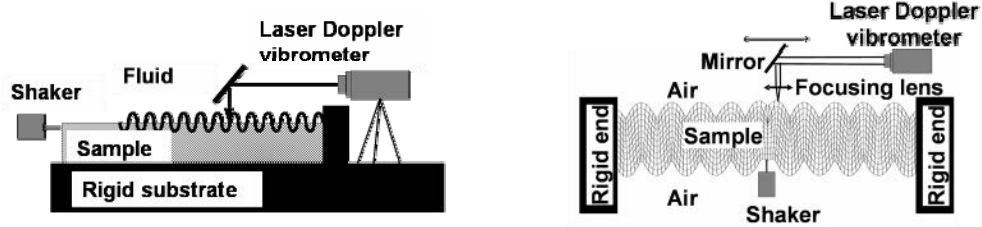


Figure 1 – Experimental setup for measuring guided waves in a poro-elastic plate backed by a rigid substrate (left) and for a plate in free conditions(right)

The maxima in the spatial spectrum correspond with the allowed propagating modes. The dispersive behaviour of the phase velocities is then obtained from the angular driving frequency and the wave number of the specific mode.

RESULTS AND DISCUSSION

Guided wave propagation in two isotropic poro-elastic plates was measured to validate the experimental principle. The measured material properties of these samples can be found in Table 1. Foam 1 is mounted in free conditions. Foam 2 was backed by a rigid substrate. The phase velocity dispersion curves are shown in figure 2. The circles indicate measured phase velocities. Clear experimental evidence was found for the existence of three guided waves propagating in a poro-elastic plate for both samples. The frequency range for which this guided wave propagation was measured exceeds that of classical quasi-static elasticity experiments.

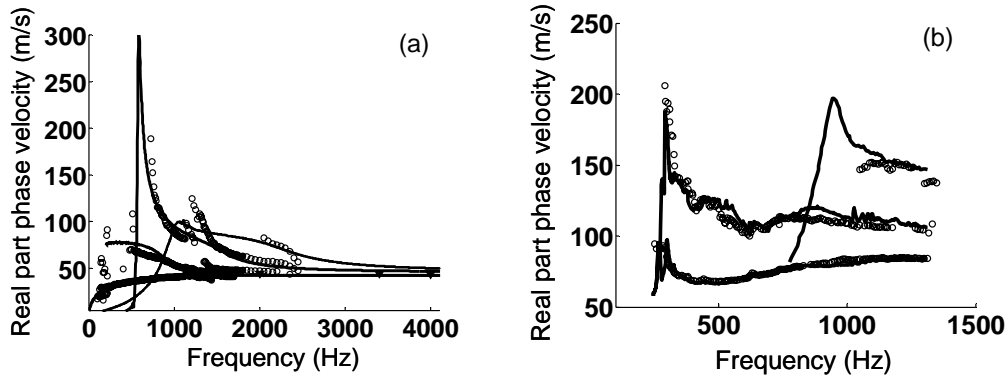


Figure 2 – Measured phase velocities (circles) of guided waves in a poro-elastic plate, Foam 1, mounted in free conditions (a) and in a poro-elastic plate, Foam 2, backed by a rigid substrate (b). The solid lines indicate the calculated phase velocity dispersion curves.

The solid lines which are presented in parts (a) and (b) of figure 3 represent the calculated phase velocity dispersion curves for a poro-elastic plate mounted in the specific boundary conditions. The phase velocity dispersion curves presented in part

(a) of figure 2 are analogous to the classical Lamb phase velocity dispersion curves. The phase velocity dispersion curves presented in part (b) of figure 2 resemble the guided waves which propagate in an elastic plate which is backed by a rigid substrate. These curves are calculated by locating the zeros of a characteristic determinant analogous to the determinants given by equation (8) and (9). The exact details of the determinants used for the calculation of the dispersive behaviour of the phase velocities in figure 2 are given in [12, 13].

The values of the parameters which are used for the calculation of the solid curves in figure 2 were measured and are given in Table 1. The phase velocities of Foam 1 (part a) were fitted best by a constant shear modulus, as indicated in Table 1.

	Foam 1	Foam 2
Tortuosity \hat{C}_i	1.4	1.01
Flow resistivity $\text{Ns/m}^4 \sigma$	130000	10500
Viscous dimension $\mu\text{m } \Lambda$	60	100
Thermal dimension $\mu\text{m } \Lambda'$	180	150
Density $\text{kg/m}^3 \rho$	59	14
Porosity ϕ	0.98	0.98
Thickness $\text{m } H$	0.04	0.02
Shear modulus $\text{kPa } N_s$	127+12.7i	Visco-elastic

The phase velocities of Foam 2 show however a clear frequency dependency which could only be accounted for by the use of a frequency dependent shear modulus. The frequency dependency of the shear modulus which was found from the measured phase velocities was already presented in figure 9 part (a) of [12]. The frequency dependency of the shear modulus was verified at low frequencies by quasi-static elasticity experiments and at high frequencies by the Rayleigh wave experiments as described by [1].

Table 1: Material properties

CONCLUSIONS

An experimental method has been presented for the measurement of the elastic behaviour of poro-elastic materials. The experimental method is based on the generation of guided waves in poro-elastic plates. A theoretical study of guided waves in TIPS layers has been presented. The proposed experimental method was validated by measuring the phase velocities of guided waves in an isotropic elastic porous material and in an isotropic visco-elastic porous material. In future research the experimental method will also be applied for studying the phase velocities of guided waves in transverse isotropic poro-elastic materials.

REFERENCES

- [1]. J. F. Allard, G. Jansens, G. Vermeir and W. Lauriks, "Frame-borne surface waves in air-saturated porous media", J. Acoust. Soc. Am. 111, 690-696 (2002).
- [2]. J. F. Allard, M. Henry, L. Boeckx, P. Leclaire and W. Lauriks, "Acoustical measurement of the shear modulus for thin porous layers", J. Acoust. Soc. Am, 117(4), 1737-1743, 2004.

- [3]. H. Deresiewicz, "The effect of boundaries on wave propagation in a liquid-filled porous solid. IV. Surface waves in a half space", Bull. Seismol. Soc. Am. 52, 627-638 (1962).
- [4]. S. Feng and D. L. Johnson, "High-Frequency acoustic properties of a fluid/porous solid interface.I. New surface mode", J. Acoust. Soc. Am. 74, 906-914 (1983).
- [5]. L. Kelders, W. Lauriks and J. F. Allard, "Surface waves above thin porous layers saturated by air at ultrasonic frequencies," J. Acoust. Soc. Am. 104, 882-889 (1998).
- [6]. W. Lauriks, L. Kelders and J. F. Allard, "Surface waves and leaky waves above a porous layer", Wave Motion 28, 57-67 (1998).
- [7]. F. C. Smith, H. Shin, K. Attenborough, "Generation of modally pure acoustic surface waves in a tapered partially filled duct," Wave Motion, 40(1), 29-40 (2005).
- [8]. L. Boeckx, P. Leclaire, C. Glorieux, W. Lauriks and J. F. Allard, "Measuring the dynamic shear modulus of poroelastic foams in the audible frequency range", Proc. International Congress in Acoustics, Kyoto 4th – 9th April 2004.
- [9]. M. A. Biot, "Theory of propagation of elastic waves in a fluid-saturated porous solid-I: low frequency range", J. Acoust. Soc. Am. 28, 168-191(1956).
- [10]. M. A. Biot, "Mechanics of deformation and acoustic propagation in porous media", J. Appl. Phys. 33, 1482-1498 (1962).
- [11]. M. D. Sharma & M. L. Gogna, "Wave propagation in anisotropic liquid-saturated porous solid", J. Acoust. Soc. Am. 90, 1068-1073 (1991).
- [12]. L.Boeckx, P. Leclaire, P. Khurana, C. Glorieux, W. Lauriks and J.F. Allard, "Investigation of the phase velocities of guided acoustic waves in soft porous layers," J.Acoust.Soc.Am, 117, 545-554, (2005).
- [13]. L.Boeckx, P. Leclaire, P. Khurana, C. Glorieux, W. Lauriks and J.F.Allard, "Guided elastic waves in porous materials saturated by air in Lamb conditions," Journal of Applied Physics, 97, (2005).

APPENDIX

$$\begin{aligned}
T_0 &= C_{11}B_5(B_7^2 - B_4B_8), \quad T_1 = T_{11} + T_{12}/c^2, \quad T_2 = T_{21} + T_{22}/c^2 + T_{23}/c^4, \\
T_3 &= T_{31} + T_{32}/c^2 + T_{33}/c^4 + T_{34}/c^6, \\
T_{11} &= C_{11}(B_4B_8 - B_7^2)\rho + C_{11}\rho B_5B_8 + 2C_{11}\rho_f B_5B_7 + C_{11}C_{33}B_4B_5 - \rho_f^2(B_4B_8 - B_7^2), \\
T_{12} &= C_{11}(2B_1 + B_2)(B_7^2 - B_4B_8) - C_{33}B_4B_5B_8 + C_{33}B_5B_7^2 + C_{11}(B_3^2B_8 + 2B_3B_5B_8) - \\
&\quad C_{11}B_6(2B_3B_7 + 2B_5B_7 - B_4B_6), \\
T_{21} &= -C_{11}\rho^2B_8 - 2C_{11}\rho\rho_fB_7 - C_{33}C_{11}\rho(B_4 + B_5) + C_{11}\rho_f^2B_5 + C_{33}\rho_f^2B_4 + \rho\rho_f^2B_8 + 2B_7\rho_f^3, \\
T_{22} &= \rho(C_{11}B_5B_8 + C_{33}B_4B_8) + \rho C_{11}(2B_1 + B_2)B_8 + 2C_{11}B_7\rho_f(2B_1 + B_2) - C_{33}\rho B_7^2 + \\
&\quad C_{11}C_{33}B_4(2B_1 + B_2) + C_{33}\rho B_5B_8 - 4\rho_f^2B_5B_8 - 2\rho_f(B_3 + B_5)(C_{11}B_6 + C_{33}B_7) - \\
&\quad 2\rho_f^2B_3B_8 - C_{11}C_{33}(B_3^2 - 2B_3B_5) + 2C_{33}\rho_fB_4B_8 + 2\rho_f^2B_6B_7 - C_{11}\rho B_6^2, \\
T_{23} &= C_{33}B_7^2(2B_1 + B_2) - (C_{11}B_5 + C_{33}B_4)((2B_1 + B_2)B_8 - B_6^2) + C_{33}(B_3 + B_5)(B_3B_8 - 2B_6B_7), \\
T_{31} &= \rho^2C_{11}C_{33} - \rho\rho_f^2(C_{11} + C_{33}) + \rho_f^4, \\
T_{32} &= \rho C_{33}\{C_{11}(B_5 + 2B_1 + B_2) - \rho B_8 - 2\rho_fB_6\} + \rho_f^2\{\rho B_8 + 2\rho_fB_6 + C_{11}(2B_1 + B_2) + C_{33}B_5\}, \\
T_{33} &= \rho C_{33}B_8(B_5 + 2B_1 + B_2) + C_{33}C_{11}B_5(2B_1 + B_2) + \rho_f^2\{B_6^2 - B_8(2B_1 + B_2)\} + C_{33}B_6(2\rho_fB_5 - \rho B_8), \\
T_{34} &= C_{33}B_5\{B_6^2 - B_8(2B_1 + B_2)\}.
\end{aligned}$$